# Diffraction by a Fractional Semi-Infinite Plate: Comparison with Impedance Boundary Conditions

*Takashi Nagasaka, Kazuma Kishiguchi, and Kazuya Kobayashi*

*Abstract* – The diffraction by a semi-infinite plate with fractional boundary conditions (FBCs) and impedance boundary conditions (IBCs) is rigorously analyzed for the E-polarized plane wave incidence using the Wiener–Hopf technique. The scattered field is evaluated with the aid of the steepest descent method, leading to a Fresnel integral representation. Numerical examples of the total field intensity are presented, and scattering characteristics of the semi-infinite plate are discussed. Comparisons of the results between the FBCs and the IBCs are also shown.

## 1. Introduction

Analysis of the diffraction by a semi-infinite plate is a fundamental and essential issue in electromagnetic theory. Recently, the diffraction problems related to fractional boundary conditions (FBCs) have been analyzed in several papers [1, 2]. Veliyev et al. studied the diffraction by a semi-infinite plate with FBC using an analytical-numerical approach and clarified the near-field behavior [2]. In a previous paper [3], we rigorously analyzed the plane-wave diffraction problem involving a semi-infinite plate with the FBCs using the Wiener–Hopf technique [4, 5] and obtained the closed-form solution.

In this article, we consider the same semi-infinite plate geometry as in the previous article [3] and carry out the Wiener–Hopf analysis of the diffraction for E-polarized plane wave incidence via the use of the FBCs. Furthermore, we will also solve the semi-infinite plate with impedance boundary conditions (IBCs) [6] using a similar procedure to the above. Comparing the results applied to the FBCs and the IBCs, we will verify the difference in scattering characteristics of the surface with the FBCs and the IBCs.

Introducing the Fourier transform of the scattered field and applying FBCs and IBCs in the transform domain, the problem is reduced to the Wiener–Hopf equations, which are solved exactly via the factorization and decomposition procedure. The scattered field in the real space is evaluated by taking the Fourier inverse of the solution in the transform domain and using the steepest descent method and the Fresnel integral representation. Numerical examples of the reflection coefficients and the field intensity are presented, and the semi-infinite plate scattering characteristics are discussed in detail. Some comparisons of the results between the FBCs and the IBCs are also given.

The time factor is assumed to be $\exp(-i\omega t)$ and suppressed throughout this article.

Manuscript received 28 December 2022.

Takashi Nagasaka, Kazuma Kishiguchi, and Kazuya Kobayashi are with the Department of Electrical, Electronic, and Communication Engineering, Chuo University, 1-13-27 Kasuga, Bunkyo-ku, Tokyo 112-8551, Japan; e-mail: nagasaka@elect.chuo-u.ac.jp, a17.87e5@g.chuo-u.ac.jp, kazuya@tamacc.chuo-u.ac.jp.

## 2. Diffraction by a Semi-Infinite Plate with FBCs

We consider the diffraction of a plane wave by a semi-infinite plate with FBCs, as shown in Figure 1. The incident field is assumed to be of E-polarization.

Let the total electric field $\phi^t(x,z)\left[\equiv E_y^t(x,z)\right]$ be

$$\phi^t(x,z) = \phi^i(x,z) + \phi(x,z) \tag{1}$$

where $\phi^i(x,z)$ is the incident field given by

$$\phi^i(x,z) = e^{-ik(x\sin\theta_0 + z\cos\theta_0)}, \quad 0 < \theta_0 < \pi/2 \tag{2}$$

In (2), $k\left[=\omega\sqrt{\mu_0\varepsilon_0}\right]$ is the free-space wavenumber, where $\varepsilon_0$ and $\mu_0$ denote the permittivity and permeability of the vacuum, respectively. The term $\phi(x,z)$ in (1) is the unknown scattered field and satisfies the two-dimensional Helmholtz equation.

The total electric field $\phi^t(x,z)$ satisfies the FBCs on the fractional semi-infinite plate as given by

$$D_x^v E_y^t(x,z)\Big|_{x=\pm 0} = 0, \quad z < 0 \tag{3}$$

where the fractional order $v$ takes the value between 0 and 1 and $D_x^v f(x)$ denotes a fractional derivative and is defined by the integral of Riemann–Liouville [7],

$$D_x^v f(x) = \frac{1}{\Gamma(1-v)}\frac{d}{dx}\int_{-\infty}^{x} f(t)(x-t)^{-v}dt \tag{4}$$

with $\Gamma(\cdot)$ being the gamma function. The reflection coefficient is given by

$$R_{FBC} = -e^{-i\pi v} \tag{5}$$

We now define the Fourier transform of the unknown scattered field $\phi(x,z)$ with respect to $z$ as

$$\Phi(x,\alpha) = (2\pi)^{-1/2}\int_{-\infty}^{\infty}\phi(x,z)e^{i\alpha z}dz \tag{6}$$

where $\alpha = \sigma + i\tau$.

For convenience of analysis, we assume the medium to be slightly lossy as in $k = k_1 + ik_2$, $0 < k_2 \ll k_1$. The solution for real $k$ is obtained by letting $k_2 \to +0$ at the end of analysis.

We introduce the polar coordinate $x = \rho\sin\theta$ and $z = \rho\cos\theta$ for $-\pi < \theta < \pi$. Rearranging the Wiener–

Hopf solution for the half-plane with the FBCs established in the previous paper [3], we can show that the scattered field $\phi(\rho,\theta)$ is reduced to an exact representation of the scattered field. The details are not discussed here, but we arrive at the exact field representation as in

$$\begin{aligned}\phi(\rho,\theta) = \frac{e^{ik\rho}}{2\pi i}\left[\int_{-\infty}^{\infty} f_1(t)e^{-k\rho t^2}dt + \int_{-\infty}^{\infty} f_2(t)e^{-k\rho t^2}dt\right] \\ - G^{s,d}(\pi-\theta_0)e^{-ik\rho\cos(|\theta|+\theta_0)}F\left[(2k\rho)^{1/2}\cos\frac{|\theta|+\theta_0}{2}\right] \\ - G^{d,s}(\pi-\theta_0)e^{-ik\rho\cos(|\theta|-\theta_0)}F\left[(2k\rho)^{1/2}\cos\frac{|\theta|-\theta_0}{2}\right]\end{aligned} \tag{7}$$

where $F(\cdot)$ is the Fresnel integral defined by

$$F(z) = e^{-i\pi/4}\pi^{-1/2}\int_z^{\infty} e^{it^2}dt \tag{8}$$

and

$$f_1(t) = \frac{G^{s,d}(w+|\theta|)\big|_{t=(2i)^{1/2}\sin(w/2)} - G^{s,d}(\pi-\theta_0)}{(2i-t^2)\cos\frac{|\theta|+\theta_0}{2} - t(1-it^2/2)^{1/2}\sin\frac{|\theta|+\theta_0}{2}} \tag{9}$$

$$f_2(t) = \frac{G^{d,s}(w+|\theta|)\big|_{t=(2i)^{1/2}\sin(w/2)} - G^{d,s}(\pi-\theta_0)}{(2i-t^2)\cos\frac{|\theta|-\theta_0}{2} - t(1-it^2/2)^{1/2}\sin\frac{|\theta|-\theta_0}{2}} \tag{10}$$

with

$$G^{s,d}(w) = \frac{\sin^{\nu}\frac{\theta_0}{2}}{\cos^{\nu}\frac{w}{2}}\left[\frac{e^{-i\pi\nu}+1}{2} \pm \frac{e^{-i\pi\nu}-1}{2}\frac{\cos\frac{w}{2}}{\sin\frac{\theta_0}{2}}\right] \tag{11}$$

$$G^{s,d}(\pi-\theta_0) = \begin{cases} e^{-i\pi\nu} \\ 1 \end{cases} \tag{12}$$

The solution (7) reduces to the exact solution with perfect electric conductor (PEC) and perfect magnetic conductor (PMC) boundary conditions when $\nu = 0$, 1.

## 3. Diffraction by a Semi-Infinite Plate with IBCs

We consider the E-polarized plane wave diffraction by a semi-infinite plate with IBCs, as shown in Figure 1.

On the surface of the semi-infinite plate, the tangential electric and magnetic field components satisfy the IBCs as given by

$$E_y^t(\pm 0,z) \pm \eta H_z^t(\pm 0,z) = 0, \quad z<0 \tag{13}$$

where $\eta$ is surface impedance. Equation (13) is also known as the Leontovich boundary condition for a planar surface [6]. The reflection coefficient is given by

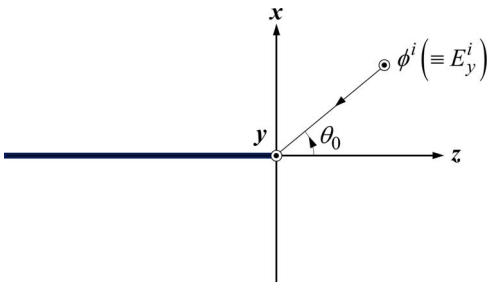


Figure 1. Geometry of the problem.

$$R_{IBC} = \frac{\eta Y_0\sin\theta_0 - 1}{\eta Y_0\sin\theta_0 + 1} \tag{14}$$

where $Y_0$ is an admittance of free space.

Using the Wiener–Hopf technique, the exact solution of the scattered field in the Fourier transform domain is obtained as

$$\Phi(x,\alpha) = \tilde{\Phi}(\alpha)e^{-\gamma|x|} \tag{15}$$

where $\gamma = (\alpha^2-k^2)^{1/2}$ and

$$\tilde{\Phi}(\alpha) = -J'_-(\alpha)/(2\gamma) \pm J_-(\alpha)/2, \quad x \gtrless 0 \tag{16}$$

with

$$J'_-(\alpha) = \frac{-(2\pi)^{-1/2}i}{M_+(k\cos\theta_0)M_-(\alpha)(\alpha-k\cos\theta_0)} \tag{17}$$

$$J_-(\alpha) = \frac{-(2\pi)^{-1/2}k\sin\theta_0}{K_+(k\cos\theta_0)K_-(\alpha)(\alpha-k\cos\theta_0)} \tag{18}$$

In (17) and (18),

$$M_{\pm}(\alpha) = (i/2)^{1/2}(k\pm\alpha)^{-1/2}N_{\pm}(\alpha) \tag{19}$$

$$K_{\pm}(\alpha) = [k/(2i\eta Y_0)]^{1/2}N_{\pm}(\alpha) \tag{20}$$

with

$$\begin{aligned}N_{\pm}(\alpha) = (1+1/\delta)^{1/2}\left\{1+\alpha^2/\left[k^2\left(\delta^2-1\right)\right]\right\}^{1/4} \\ \cdot\exp\left\{-\frac{\delta}{\pi}\int_{\pi/2}^{\arccos(\pm\alpha/k)}\frac{t\cos t}{\sin^2 t-\delta^2}dt\right. \\ \pm\frac{i}{2\pi}\ln\left[\delta+\left(\delta^2-1\right)^{1/2}\right] \\ \left.\cdot\ln\left[\frac{ik\left(\delta^2-1\right)^{1/2}+\alpha}{ik\left(\delta^2-1\right)^{1/2}-\alpha}\right]\right\}\end{aligned} \tag{21}$$

$$\delta = 1/(\eta Y_0). \tag{22}$$

The scattered field in the real space is obtained by taking the inverse Fourier transform of (15) according to the formula

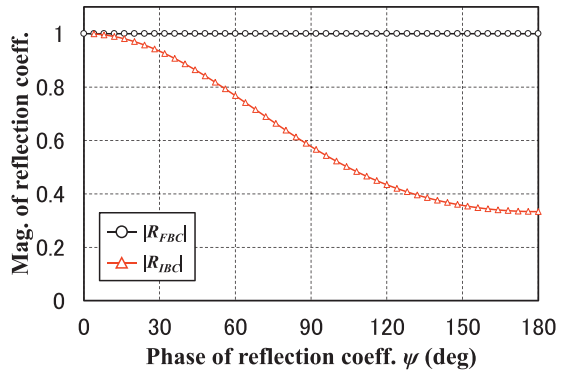


Figure 2. Magnitude of $R_{FBC}$ and $R_{IBC}$ versus phase of reflection coefficient $\psi$, where $\theta_0 = 60^\circ$ and $\mathrm{Re}\eta = 1/(2Y_0 \sin\theta_0)$.

$$\phi(x,z) = (2\pi)^{-1/2} \int_{-\infty+ic}^{\infty+ic} \tilde{\Phi}(\alpha) e^{-\gamma|x| - i\alpha z} d\alpha \tag{23}$$

where $-k_2 < c < k_2 \cos\theta_0$.

We introduce the polar coordinate $x = \rho \sin\theta$ and $z = \rho \cos\theta$ for $-\pi < \theta < \pi$ and let $k_2 \to +0$. Using the steepest descent method [8], we can show after some manipulations that (23) is reduced to the Fresnel integral representation,

$$\begin{aligned}\phi(\rho,\theta) \sim\ & -h(\theta,\theta_0,\eta) e^{-ik\rho\cos(|\theta|+\theta_0)} F\left[(2k\rho)^{1/2} \cos\frac{|\theta|+\theta_0}{2}\right] \\ & - h(\theta,\theta_0,\eta) e^{-ik\rho\cos(|\theta|-\theta_0)} F\left[(2k\rho)^{1/2} \cos\frac{|\theta|-\theta_0}{2}\right] \\ & + H(|\theta| - \pi + \theta_0) e^{-ik\rho\cos(|\theta|+\theta_0)} \\ & \cdot \left[h(\theta,\theta_0,\eta) - \frac{1 \mp \eta Y_0 \sin\theta_0}{1 + \eta Y_0 \sin\theta_0}\right], \quad x \gtrless 0 \end{aligned} \tag{24}$$

under the condition that $|k|\rho$ is not too small, where $F(\cdot)$ is the Fresnel integral defined by (8) and

$$h(\theta,\theta_0,\eta) = -\frac{1 - 2\eta Y_0 \sin\frac{\theta_0}{2} \sin\frac{\theta}{2}}{N_+(k\cos\theta_0) N_+(k\cos\theta)} \tag{25}$$

$$\begin{aligned} H(\xi) &= 1, \quad \xi > 0, \\ &= 0, \quad \xi < 0 \end{aligned} \tag{26}$$

## 4. Numerical Results and Discussion

We compare the reflection coefficients $R_{FBC}$ in (5) and $R_{IBC}$ in (14). Figures 2 and 3 show the amplitudes, fractional order $v$, and surface impedance $\eta$ as a function of phase of reflection coefficient $\psi$ for $R_{FBC}$ and $R_{IBC}$, where $\theta_0 = 60^\circ$. The term $\eta$ satisfies the following conditions for the phase of reflection coefficient $\psi$:

$$|\mathrm{Re}\eta| < 1/(Y_0 \sin\theta_0) \tag{27}$$

$$\mathrm{Im}\eta = \frac{\cos\psi + \left[1 - (Y_0 \sin\theta_0 \sin\psi \mathrm{Re}\eta)^2\right]^{1/2}}{Y_0 \sin\theta_0 \sin\psi} \tag{28}$$

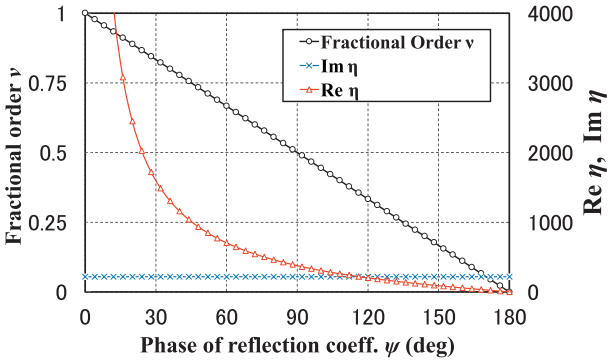


Figure 3. Fractional order $v$ and surface impedance $\eta$ versus phase of reflection coefficient $\psi$ for $R_{FBC}$ and $R_{IBC}$, where $\theta_0 = 60^\circ$ and $\mathrm{Re}\eta = 1/(2Y_0 \sin\theta_0)$.

We have chosen $\mathrm{Re}\eta = 1/(2Y_0 \sin\theta_0)$ in these calculations. It is seen from the figures that fractional order $v$ is proportional to phase of reflection coefficient $\psi$. We also observe that $|R_{FBC}|$ is constant when $\psi$ is changed.

We present some numerical examples of the total field intensity and discuss the scattering characteristics of the semi-infinite plate with the FBCs and the IBCs. The normalized total field intensity is introduced as

$$\left|\phi^t(\rho,\theta)\right|[\mathrm{dB}] = 20\log_{10}\left[\frac{\left|\phi^t(\rho,\theta)\right|}{\max\limits_{|\theta|\le\pi}\left|\phi^t(\rho,\theta)\right|}\right] \tag{29}$$

Figures 4 and 5 show numerical examples of the total field intensity as a function of observation angle $\theta$, where the incidence angle is fixed as $\theta_0 = 60^\circ$ and the distance from the origin $\rho$ is $\lambda$ ($\lambda$: wavelength). We have chosen the fractional order $v$ and the surface impedance

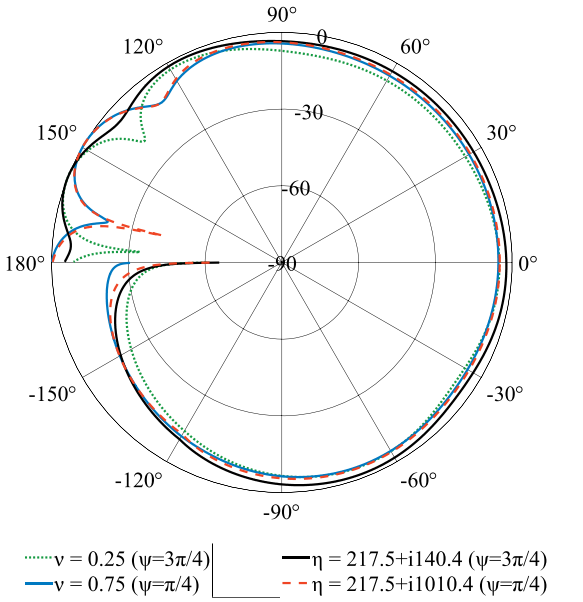


Figure 4. Total electric field $\left|\phi^t(\rho,\theta)\right|$[dB] versus observation angle $\theta$ for $\theta_0 = 60^\circ$, $\rho = \lambda$, $\psi = 3\pi/4$, $\pi/4$.

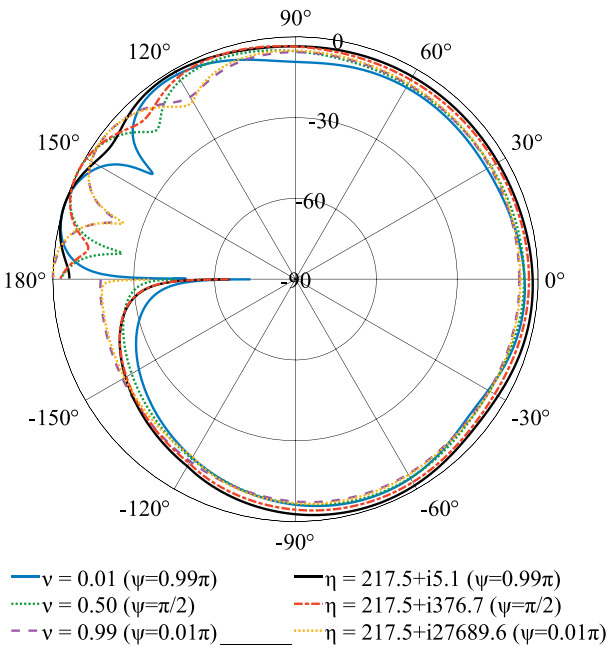


Figure 5. Total electric field $|\phi^t(\rho,\theta)|$ [dB] versus observation angle $\theta$ for $\theta_0 = 60^\circ$, $\rho = \lambda$, $\psi = 0.99\pi$, $\pi/2$, $0.01\pi$.

$\eta$, referring to Figure 3, where the phase of reflection coefficient $\psi = 3\pi/4$, $\pi/4$ and $\psi = 0.99\pi$, $\pi/2$, $0.01\pi$, respectively. In Figures 4 and 5, we observe by comparing the results for the FBCs and the IBCs having the same $\psi$ that the peak locations of the total field intensity exhibit close features over the whole ranges. We also see that, the magnitude of the results for the FBCs and the IBCs having the same $\psi$ show good agreement when approaching $\psi \to 0$ (PMC). On the other hand, the results become very different when $\psi$ approaches $\pi$ (PEC).

## 5. Conclusions

In this article, we have solved exactly the plane wave diffraction by a semi-infinite plate with the FBCs and the IBCs for E polarization using the Wiener–Hopf technique. We have obtained the exact solution to the Wiener–Hopf equations. The scattered field has been derived with the aid of the steepest descent method, leading to a Fresnel integral representation. We have carried out the numerical computation of the reflection coefficients for the FBCs and the IBCs and the normalized field intensity. We have investigated the scattering characteristics of the semi-infinite plate with the FBCs and the IBCs.

## 6. Acknowledgments

This work is partly supported by the Murata Science Foundation and the 2022 Chuo University Overseas Research Program.

## 7. References

1. E. I. Veliev, M. V. Ivakhnychenko, and T. M. Ahmedov, "Fractional Boundary Conditions in Plane Wave Diffraction on a Strip," *Progress in Electromagnetics Research*, **79**, January 2008, pp. 443-462.
2. E. Veliyev, V. Tabatadze, K. Karaçuha, and E. Karaçuha, "The Diffraction by the Half-Plane With the Fractional Boundary Condition," *Progress in Electromagnetics Research M*, **88**, January 2020, pp. 101-110.
3. T. Nagasaka and K. Kobayashi, "Plane Wave Diffraction by a Semi-Infinite Plate With Fractional Boundary Conditions," *URSI Radio Science Letters*, **3**, December 2021, doi: 10.46620/21-0042.
4. R. Mittra and S. W. Lee, *Analytical Techniques in the Theory of Guided Wave*, New York, Macmillan, 1971.
5. B. Noble, *Methods Based on the Wiener-Hopf Technique for the Solution of Partial Differential Equations*, London, Pergamon, 1958.
6. T. B. A. Senior, "Impedance Boundary Conditions for Imperfectly Conducting Surfaces," *Applied Scientific Research, Section B*, **8**, 1960, pp. 418-436.
7. S. G. Samko, A. A. Kilbas, and O. I. Marichev, *Fractional Integrals and Derivatives: Theory and Applications*, Langhorne, PA, Gordon and Breach Science Publishers, 1993.
8. K. Kobayashi, "Wiener-Hopf and Modified Residue Calculus Techniques," in E. Yamashita (ed.), *Analysis Methods for Electromagnetic Wave Problems*, Boston, Artech House, 1990, Chapter 8.